

DI-3-n-butylphthalide mitigates stress-induced cognitive deficits in mice through inhibition of NLRP3-Mediated neuroinflammation

Xiu Chen^{a,1}, Juan-Ling He^{a,1}, Xue-Ting Liu^{a,1}, Na Zhao^a, Fan Geng^a, Meng-Meng Zhu^a, Gong-Ping Liu^{c,d,**}, Qing-Guo Ren^{b,*}

^a School of Medicine, Southeast University, Nanjing, 210009, China

^b Department of Neurology, Affiliated ZhongDa Hospital of Southeast University, Nanjing, 210009, China

^c Department of Pathophysiology, Tongji Medical College, Huazhong University of Science and Technology, Wuhan, 430030, China

^d Co-innovation Center of Neurodegeneration, Nantong University, Nantong, 226019, China

ARTICLE INFO

Keywords:

DI-3-n-Butylphthalide
Chronic stress
Cognitive deficits
NLRP3 inflammasome

ABSTRACT

Our previous study has demonstrated that chronic stress could cause cognitive deficits and tau pathology. However, the underlying mechanism and whether/how DI-3-n-Butylphthalide (NBP) ameliorates these effects are still unclear. Here, Wild-type mice were subjected to chronic unpredictable and mild stress (CUMS) for 8 weeks. Following the initial 4 weeks, the stressed animals were separated into susceptible (depressive) and unsusceptible (resilient) groups based on behavioral tests. Then, NBP (30 mg/kg i.g) was administered for 4 weeks. Morris water maze (MWM), Western-blot, Golgi staining, immunofluorescence staining and ELISA were used to examine behavioral, biochemical, and pathological changes. The results showed that both depressive and resilient mice displayed spatial memory deficits and an accumulation of tau in the hippocampus. Activated microglia and NLRP3 inflammasome were found after 8-week chronic stress. We also found a decreased level of postsynaptic density (PSD) related proteins (PSD93 and PSD95) and decreased the number of dendritic spines in the hippocampus. Interestingly, almost all the pathological changes in depressive and resilient mice previously mentioned could be reversed by NBP treatment. To further investigate the role of NLRP3 inflammasome in chronic stress-induced cognitive deficits, NLRP3 KO mice were also exposed to chronic stress. And these changes induced by chronic stress could not be found in NLRP3 KO mice. These results show an important role for the NLRP3/caspase-1/IL-1 β axis in chronic stress-induced cognitive deficits and NBP meliorates cognitive impairments and selectively attenuates phosphorylated tau accumulation in stressed mice through regulation of NLRP3 inflammatory signaling pathway.

1. Introduction

Chronic stress refers to the harmful effects when the body is stimulated by various adverse factors. The long-term and repeated stimulation of chronic stress accelerates brain aging and various mental illnesses, including lower immune function, depressive disorder, bipolar disorder, and dementia (Sanacora et al., 2022; Russell and Lightman, 2019). It has been established that people with all mental disorders were strong independent risk factors for accidental death with a 6.3-fold risk of accidental death among men and a 5.3-fold risk among women (Crump et al., 2013). Various evidence from preclinical and clinical studies have

demonstrated the correlation between chronic stress and memory decline, also known as stress-induced cognitive deficits (SICD) (Kim and Diamond, 2002; Wilson et al., 2003). The most important thing is that chronic stress can cause the occurrence and development of cognition impairment. Studies have shown that chronic stress is a strong risk factor for cognitive impairment and has a key role in hastening pathology and neurodegeneration in Alzheimer's disease (Greenberg et al., 2014).

Neuroinflammatory processes play a crucial part in the occurrence and progression of dementia (Bhattacharya et al., 2016) as well as depression (Knezevic and Mizrahi, 2018). Several studies suggest that there is a relationship between SICD and neuroinflammation (McKim

* Corresponding author. Department of Neurology, Affiliated ZhongDa Hospital, School of Medicine, Southeast University, Nanjing, Jiangsu, 210009, China.

** Corresponding author. Department of Pathophysiology, Tongji Medical College, Huazhong University of Science and Technology, Wuhan, 430030, China.

E-mail addresses: liuggp111@hotmail.com (G.-P. Liu), renqingguo1976@163.com (Q.-G. Ren).

¹ These authors contributed equally to this work.

et al., 2016). Both in depression (Setiawan et al., 2015) and Alzheimer's disease, proliferation and activation of microglia could be observed obviously (Knezevic and Mizrahi, 2018). NLRP3 inflammasome, a tripartite protein of the nucleotide-binding domain and leucine-rich repeat (NLR) family, is the best characterized inflammasome complex within the central nervous system (Heneka et al., 2018). Moreover, chronic unpredictable and mild stress (CUMS) can trigger NLRP3 inflammasome activation, associated with microglial activation, interleukin-1beta (IL-1 β) secretion (Lu et al., 2014). However, whether the activation of NLRP3 inflammasome is involvement in the mechanism of SCID remains unclear.

Different from traditional antidepressants (SSRI and SNRI, etc.), Di-3-n-butylphthalide (NBP), an emerging brain-protective drug in China, is a natural compound with significant biological activity isolated from celery seeds. It is a lipid-soluble and a small molecule drug that can directly pass through the blood-brain barrier (Xiang et al., 2021). Since being approved by the National Medical Products Administration (NMPA) in 2004, NBP has shown a great therapeutic interest for acute ischemic stroke on improving neurological deficits, with good safety and tolerability (Fan et al., 2021). Recent studies have proved that NBP as well as its derivatives and analogs (NBP_s) have the effects of anti-neuroinflammation, anti-depressant, inhibiting neuronal apoptosis, ameliorating diabetes-associated cognitive decline and ameliorating brain nerve function (Marco-Contelles and Zhang, 2020; Wu et al., 2020; Wang et al., 2021). And NBP has been reported to direct APP processing toward a non-amyloidogenic pathway and preclude A β formation in the 3xTg-AD mice, which are important processes involved in learning and memory (Peng et al., 2010). These data determine a multitarget neuroprotective function for NBP. However, until now, few experimental studies evaluate the therapeutic effect of NBP in patients with stress-induced cognitive dysfunction. NBP treatment could rescue dopaminergic neurons by reducing NLRP3 inflammasome activation and ameliorating mitochondrial impairments in Parkinson's disease (Que et al., 2021). In addition, Liu X et al. demonstrated that NBP abated the levels of NLRP3, IL-1 β , and caspase-1 in acute cerebral ischemia, indicating that NBP can inhibit the inflammatory response induced by NLRP3 (Liu et al., 2021). Substantial studies confirm that NLRP3 inflammasome plays a critical role in the regulation of neuroinflammation (Wu et al., 2021). Importantly, the pathogenesis of SCID involved inflammatory responses, disorder of vasoconstriction and relaxation in mice and humans, which are the action targets of NBP (Barrett et al., 2021; DiSabato et al., 2021; Gao et al., 2022), suggest that NBP maybe play a pivotal role in the protection of SCID.

Based on the above-mentioned data, in this study, we hypothesized that NBP may have therapeutic efficacy for stress-induced cognitive deficits through inhibiting NLRP3/caspase-1-mediated neuroinflammation. We used the chronic stress mice model to analyze the improvement effect and mechanism of NBP therapy on behavioral functions and pathology and tested whether inhibition of NLRP3 could reverse the detrimental consequences on cognitive function and structural plasticity in mice, aiming to provide theoretical support for the clinical applying of NBP in the treatment of patients with stress-induced cognitive impairment.

2. Materials and methods

2.1. Animals

Male NLRP3 KO mice and wild-type mice (8 weeks old) with C57BL/6 background were purchased from the Jackson Laboratory, experimental Animal Center (Shanghai, China). After arrival, the mice were housed in a temperature and humidity-controlled animal experiment laboratory with a 12-h light/dark cycle (lights on at 7:00 a.m.), and standard laboratory water and chow were provided randomly. To reduce environmental effects, those mice were allowed to adapt to laboratory conditions for 2 weeks before use.

The experimental procedures involving animals were performed by the ARRIVE (Animal Research: Reporting of In Vivo Experiments) guidelines (Percie du Sert et al., 2020; Karp et al., 2015), and approved by the Animal Experimental Ethical Inspection Form of Southeast University.

2.2. Time course and experimental design

Fig. 1A showed the timetable of behavioral test, and brain tissue analysis of stressed mice. The mice (2 months old) first adapted to the environment for 2 weeks and were exposed to seven different stressors for 8 weeks. From the 4th week, two group of mice received NBP (30 mg/kg, i.g, quaque die) treatment for 4 weeks. Importantly, at the beginning of week 4 and the end of week 8, all mice underwent a series of behavioral tests to evaluate their emotional and cognitive functions. Then, brain tissues were collected and processed for biochemical tests.

2.3. Chronic unpredictable stress paradigm

After a survival period of 10 weeks, the mice were subject to 8 weeks of CUMS as described in detail previously by us and Lotan A et al. (Wu et al., 2018a; Lotan et al., 2018). The CUMS included seven different stressors, including deprivation of food and water (12 h), empty cage (12 h), tilted cage (14 h), nip-tail (1 min), light-dark cycle reversal, cold environment (5 min), and restraint in a bottle (1 h). To avoid habituation, stressors were randomly selected every week and each animal received the same number of stressors at the end of the experiments.

On the day of the behavioral test, test procedures were executed from 10:00 a.m. to 4:00 p.m. Dim light (20 lux) was used in the room during the behavioral test.

2.4. Behavioral tests

2.4.1. Sucrose preference test

The sucrose preference test (SPT) was applied to detect stress-induced anhedonia in mice (Liu et al., 2018). After the last stressor, the animals were individually housed and acclimated to the 1% sucrose solution(w/v) over 48 h. Then, mice were given two bottles for 24 h with the right/left location balanced, one of which contained tap water and the other 1% sucrose. The position of the two bottles was switched every 6h to avoid potential location preference on drinking water. The 24h consumption of water and the sucrose solution was measured. The preference ratio (%) for sucrose = sucrose solution intake/(sucrose solution intake + water intake) \times 100%.

2.4.2. Forced swimming test

The forced swimming test (FST) is divided into two phases: pre-test and test phase (Porsolt et al., 1977). The mice were gently and individually placed in a cylinder (30 \times 60 cm) filled with freshwater (22–25 $^{\circ}$ C, 30-cm deep) 24 h before the experiment. The test duration was 6 min. And during the 6-min test, the immobility time in the last 5 min was quantified by an investigator unaware of animal grouping. The mice were considered immobile after no additional activity was observed, except for a certain slightly moving to keep their nose above the surface. The mice were removed after 5 min, dried, and returned to their original cage. Water was changed after each test.

2.4.3. Morris water maze

The Morris water maze (MWM) was used to determine animals' spatial learning and referential memory ability, based on a protocol (Vorhees and Williams, 2006). Clean water was maintained at 25 \pm 2 $^{\circ}$ C in a black circular pool (120 cm in diameter). 4 months old NLRP3 $-/-$ mice and wild-type mice were trained to find the platform using a visible marker. One of the four quadrants of the water tank was chosen as the target quadrant to place an escape platform (11 cm in diameter, 1.5 cm below the surface) with opaque water dyeing with a white additive.

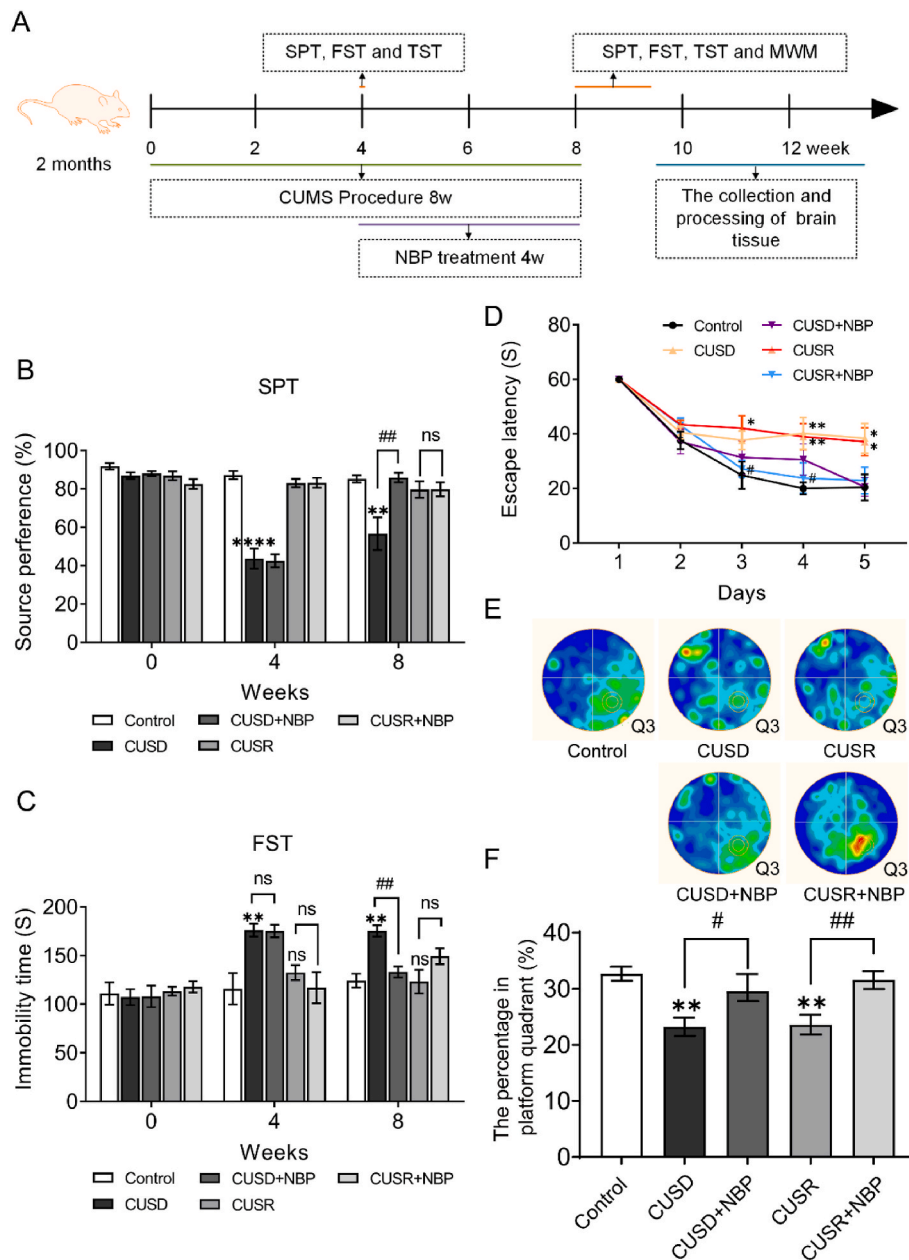


Fig. 1. NBP ameliorated behavioral changes in CUMS mice

A. An overview of the experimental design. B–C. Measurement of depressive behavior by SPT and FST. (n = 7, 10, 9, 9, and 9 for group Con, CUSD, CUSD + NBP, CUSR, and CUSR + NBP mice respectively. SPT: 4W [Con CUSD] ****P < 0.0001, [Con CUSR] ****P < 0.0001, [CUSD CUSD + NBP] P = 0.9995, [CUSR CUSR + NBP] P = 0.9999, 8W: [Con CUSD] **P = 0.0053, [Con CUSR] P = 0.9532, [CUSD CUSD + NBP] ##P = 0.0018, [CUSR CUSR + NBP] P = 0.9999, FST: 4W: [Con CUSD] **P = 0.0043, [Con CUSR] P = 0.8413, [CUSD CUSD + NBP] P > 0.99, [CUSR CUSR + NBP] P > 0.99, 8W: [Con CUSD] **P = 0.09, [Con CUSR] P > 0.99, [CUSD CUSD + NBP] ##P = 0.0043, [CUSR CUSR + NBP] P = 0.1715) D–F. Spatial learning and memory test using the acquisition phase. (D) Probe test at consecutive 6 days. (E, F) MWM test in consecutive 5 days. (n = 7, 9, 9, 9, and 9 for group Con, CUSD, CUSD + NBP, CUSR, and CUSR + NBP mice respectively. Escape latency: day3 [Con CUSD] *P = 0.0418, [Con CUSR] *P = 0.021, day4 [Con CUSD] **P = 0.0056, [Con CUSR] **P = 0.0081, [CUSD CUSD + NBP] P = 0.248, [CUSR CUSR + NBP] *P = 0.0418, day5 [Con CUSD] *P = 0.0184, [Con CUSR] *P = 0.0283, [CUSD CUSD + NBP] #P = 0.0202, [CUSR CUSR + NBP] P = 0.0585. The percentage in platform quadrant (%): [Con CUSD] **P = 0.0019, [Con CUSR] **P = 0.0023, [CUSD CUSD + NBP] #P = 0.020, [CUSR CUSR + NBP] ##P = 0.047. *P < 0.05, **P < 0.01, ***P < 0.001, ****P < 0.0001, #P < 0.05, ##P < 0.01, ###P < 0.0001. *P versus Con group, #P versus CUSD or CUSR group. All data are represented by the mean ± SEM. One-way ANOVA with Tukey’s multiple comparisons test.)

During the exploration trials, mice were trained to seek hidden platforms in the water tank based on spatial cues (four sequential trials per day for five days). The mice facing the wall of the pool were put into the water from the strike mark in each quadrant at random. Each quadrant had an equal chance of winning. During each training session, mouse movement was permitted for 60 s at a time. The mouse was allowed to remain on the platform for 30 s when it was found. If the mouse cannot find the platform within 60 s, it would be guided to the platform to rest for 30 s. Each test interval was at least 30 min. After each experiment, the mice were gently dried and returned to their cages with a heating lamp. On the sixth day, mice were tested in a maze without a platform to test their spatial memory. Each mouse swam for 60 s free in the pool. Both NLRP3 $-/-$ mice and wild-type mice showed the same swimming distance in the probe test and normal acquisition of visible platform. Our computerized tracking system monitored the mouse escape latencies, time spent in the target quadrant, and swimming paths for statistical analysis.

2.5. Tissue collection

The animals were first put through a behavioral test. A few days after the completion of the behavioral evaluation, the animal will be executed by CO2 inhalation after sevoflurane anesthesia, and brain tissues will be collected for other tests. Then, brains were obtained and stored at -80°C for further analysis.

2.6. Golgi staining and dendritic spine analysis

The Golgi staining procedure was executed in the mouse using the FD Rapid Golgi Stain kit (FD NeuroTechnologies). The brains were immersed in solutions A and B for 2 weeks at room temperature before being transferred to solution C at 4°C for 24 h. The dorsal hippocampus, prefrontal cortex, and ventral hippocampus were studied. The neurons in each region of the mouse were randomly selected. We randomly selected two segments, one from the apical oblique dendrite (AO) and one from the basal shaft (BS) dendrite. Since the dendritic spine density

was revealed blindly, the density of the spines was determined.

2.7. Western-blot

The whole brain was placed on ice and washed with 0.1M PBS solution (pH 7.4). The hippocampal region was immediately and gently isolated. Then, the hippocampal tissues were homogenized in lysis buffer under pre-cooled RIPA lysate mixed with aprotinin, Phenylmethanesulfonyl fluoride (PMSF), and protease inhibitor (Beyotime Biotechnology, Shanghai, China). Protein concentration in the supernatant collected after centrifugation (4 °C; 13,000g; 20 min) is determined using a BCA kit (Beyotime Biotechnology, Shanghai, China). Protein samples were diluted 5:1 with sample loading buffer (6 concentrates; Beyotime, China), then boiled for 10 min at 100 °C, and stored at −20 °C. The proteins were separated on 4%–20% SDS-PAGE, transferred to polyvinylidene difluoride membranes (PVDF, Immobilon Transfer Membrane, Millipore, USA), and probed with the indicated primary antibodies and secondary antibodies conjugated with horseradish peroxidase. A chemiluminescence assay (ECL, Millipore, Billerica, Massachusetts, USA) was used to detect antigens, followed by an analysis of optical density using Image Pro-Plus 6.0 software. The average background density was subtracted, and integrated optical density values were determined.

The primary antibodies were as follows: anti-tau (p-S396) (1:5000; Abcam), anti-tau (p-T231) (1:5000; Abcam), anti-tau-1 (1:1000; Millipore), anti-tau-5 (1:2000; Abcam), Phospho-mTOR (Ser2448) (1:1000; CST). Internal control was performed using Beta Actin (β -actin) antibody (1:5000; Proteintech) or GAPDH (1:2000; Cell Signaling). Incubation of the membranes with anti-nlrp3(1:2000; CellSignaling), caspase-1(1:500; Santa), IL-1 β (1:2000; Abcam), PSD95 (1:2000; Abcam), PSD93 (1:2000; Abcam), NR1(1:2000; Abcam). The secondary antibodies were as follows: Goat anti-rabbit or Goat anti-mouse (1:5000; Proteintech, China).

2.8. Immunofluorescence

Hippocampal tissues were fixed with 4% paraformaldehyde and infiltrated with 0.3% Triton X-100. The nonspecific binding sites were blocked with 5% bovine serum albumin (BSA). Tissues were incubated with primary antibodies (Iba1, 1:200, Wako), and then incubated with fluorescein isothiocyanate-conjugated secondary antibodies. The nuclei were stained by DAPI (Solarbio) and images were captured using a confocal microscope (OLYMPUS FV3000, Japan).

2.9. Quantitative and statistical analyses

Graph Pad Prism 9.0 software was used for statistical analyses. One-way analysis of variance (ANOVA) with Tukey's multiple comparisons test was used to analyze the difference between the means of more than two groups. Two-way ANOVA with Bonferroni's multiple comparisons test was used for multiple comparisons between groups when assessing the effect of stress on genotype. All the data in this study were presented as mean \pm standard error of the mean (SEM). The statistical significance level of any measurement was set at * $p < 0.05$, ** $p < 0.01$, *** $p < 0.001$ and **** $p < 0.0001$ using two-tailed tests.

3. Results

3.1. NBP ameliorated behavioral changes in CUMS mice

The experimental process is shown in Fig. 1A. The SPT was used to investigate anhedonia (Fig. 1B). No significant difference was found in sucrose preference among the groups before the experiment (week 0). After 4 weeks of CUMS, 61% of the mice showed anhedonic or depressive-like behavior (CUSD), while the remaining 39% of mice were considered to be nonanhedonic or resilient to CUMS (CUSR). Compared to the control, the CUSD group showed significantly decreased sucrose

preference at week 4 and 8. NBP significantly increased the sucrose preference in CUSD mice. There were no significant differences between control, CUSR, and CUSR treated with NBP in sucrose preference. FST was also used to evaluate CUMS mice (Fig. 1C). In this study, CUSD mice showed significantly increased immobility time in the FST at week 4 and 8. These manifestations could be reversed by NBP. There were no significant differences between control, CUSR, and CUSR treated with NBP in FST.

MWM was used to detect the spatial learning and memory retention of the mice. Interestingly, during the training period, the latency to the hidden platform both in the CUSD and CUSR mice was longer than that in the control on the third day, fourth day, and fifth day (Fig. 1D). NBP could apparently restore the performance both in all stressed mice (Fig. 1D). To study memory retention, the mice were subjected to a probe trial in which the platform was removed 24 h after the training session. Mice exposed to chronic stress spent significantly less time exploring in the target quadrant, regardless of whether the mice were CUSD or CUSR (Fig. 1E and F). Notably, NBP alleviated long-term memory deficits (24-h probe) in CUSD and CUSR mice compared with the control, as determined by the significant increase in the duration of time spent in the Q3 quadrant (Fig. 1E and F).

3.2. Effect of NBP on chronic stress-induced tau alteration in the hippocampus in mice

Here, we measured tau level in the hippocampus using western-blot. The immune-reactivity of tau at Thr-231, Ser-396 and Ser-198, 199, 202 site epitope were increased in CUSD and CUSR group compared with those of the control (Fig. 2A–D). Accordingly, an increased level of total tau (Tau-5) was found in the hippocampus in all stressed mice (Fig. 2A, E). After 4 weeks treatment with NBP, the levels of phosphorylated tau, nonphosphorylated tau, and total tau (shown by the immunoreactivity of tau at Ser-396 site, at Thr-231 site, at tau-1 epitope, and tau-5 epitope respectively) were evidently reversed in the CUSD and CUSR mice compared with those of the control (Fig. 2A–E). Our results suggested that NBP could both decrease phosphorylated and nonphosphorylated tau accumulation in the hippocampus of stressed mice. As the accumulated tau is hyperphosphorylated at some of the GSK-3 favorite sites during CUMS stimulation (Ning et al., 2018; Wu et al., 2018b), we studied the involvement of GSK-3. The level of serine-9-phosphorylated GSK-3 β (inactive form) was decreased after CUMS in mice, which could be reversed by NBP treatment. The total level of GSK-3 β was not changed (Fig. 2F and G).

3.3. NBP suppressed NLRP3 inflammasome activation in chronic stress mice

The protein expression of NLRP3, Caspase-1 P20, IL-1 β significantly increased in the CUSD and CUSR compared to the control group detected by western-blot (Fig. 3A–D). The activated microglia in the hippocampus of CUSD and CUSR mice was obvious showed by immunofluorescence staining (Fig. 3E and F). Both expression of NLRP3, Caspase-1 P20, IL-1 β and Iba-1 positive cell could be reversed by NBP treatment (Fig. 3A–F).

3.4. NBP ameliorates synaptic plasticity impairment caused by chronic stress

Synaptic associated proteins are closely related to the structure and function of synapses. The synaptic associated protein expression was detected by western-blot in the hippocampus (Fig. 4A). Compared with the control, the protein PSD93 and PSD95 expression of CUSD and CUSR was significantly decreased, NBP treatment increased the protein PSD93 and PSD95 levels of CUSD and CUSR (Fig. 4A–C). Synaptophysin protein levels were not significantly changed among these groups (Fig. 4A, D).

Dendritic spine structure in the hippocampus was detected by Golgi

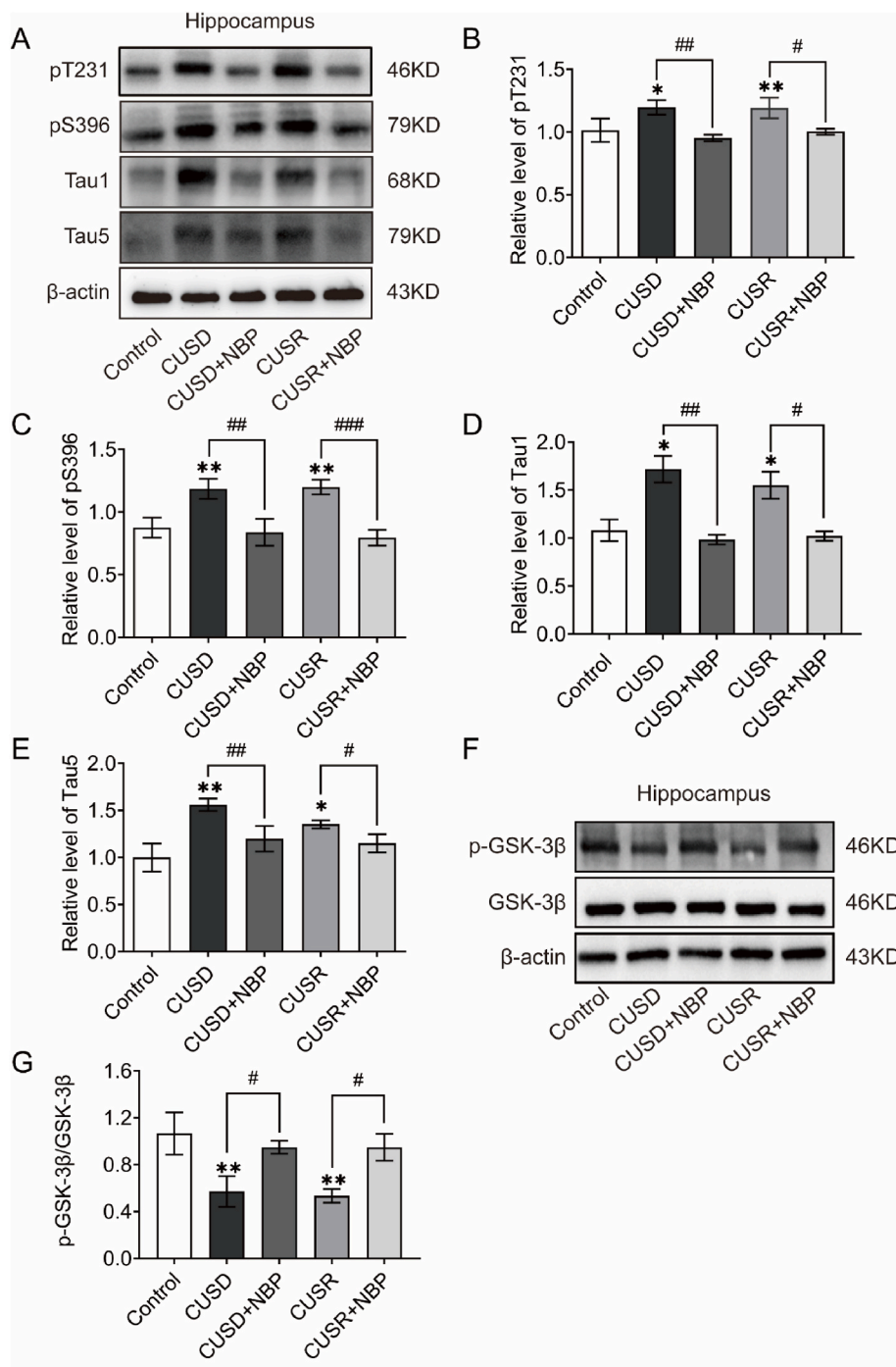


Fig. 2. Effect of NBP on chronic stress-induced tau alteration in the hippocampus in mice

A-E. Western blot and quantification of pT231, pS396, Tau-1, Tau-5, p-GSK-3β, and GSK-3β in the hippocampus lysates. (n = 3, 3, 3, 3, and 3 for group Con, CUSD, CUSD + NBP, CUSR, and CUSR + NBP mice respectively. pT231: [Con CUSD] *P = 0.0229, [Con CUSR] **P = 0.0092, [CUSD CUSD + NBP] ##P = 0.0032, [CUSR CUSR + NBP] #P = 0.0147. pS396: [Con CUSD] **P = 0.0054, [Con CUSR] **P = 0.0040, [CUSD CUSD + NBP] ##P = 0.0024, [CUSR CUSR + NBP] ###P = 0.0007. Tau-1: [Con CUSD] *P = 0.0138, [Con CUSR] *P = 0.0137, [CUSD CUSD + NBP] #P = 0.046, [CUSR CUSR + NBP] #P = 0.0149. Tau5: [Con CUSD] **P = 0.0067, [Con CUSR] *P = 0.0284, [CUSD CUSD + NBP] ##P = 0.0079, [CUSR CUSR + NBP] #P = 0.0342. p-GSK-3β/GSK-3β: [Con CUSD] **P = 0.0030, [Con CUSR] **P = 0.0018, [CUSD CUSD + NBP] #P = 0.0184, [CUSR CUSR + NBP] #P = 0.0101. *P < 0.05, **P < 0.01, #P < 0.05, ##P < 0.01, ###P < 0.001. All data are represented by the mean ± SEM. *P versus Con group, #P versus CUSD or CUSR group. All data are represented by the mean ± SEM. One-way ANOVA with Tukey's multiple comparisons test.).

staining. We found that the AO and BS spine densities were significantly lower in CUSD and CUSR group than those in the wild type group, however, NBP could significantly increase the AO and BS spine densities in the hippocampus of stressed mice (Fig. 4E–G).

3.5. The cognitive and pathological alteration in NLRP3 KO mice after CUMS

MWM was used to evaluate the spatial learning and memory retention in NLRP3 KO mice after CUMS. During the 5-day training process, the CUMS mice exhibited significantly prolonged times in finding the hidden platform on days 4 and 5 (Fig. 5A). No difference was found in training period among NLRP3 KO mice with or without CUMS and

normal control (Fig. 5A). On the 6th day, different from wild-type mice, stressed NLRP3 KO mice also performed as well as NLRP3 KO mice control (Fig. 5A and B).

Protein levels of NLRP3, caspase-1p20 and IL-1β were detected by western-blot. In accordance with our above-mentioned results, NLRP3, caspase-1p20 and IL-1β levels were increased in the hippocampus of wild-type mice apparently following CUMS (Fig. 5C–F). No significant difference was found in NLRP3, caspase-1p20 and IL-1β levels between stressed or non-stressed NLRP3 KO mice (Fig. 5C–F).

Tau protein was measured by western-blot. Compared with the normal control, an increased level of total tau and phosphorylated tau were found in the hippocampus in stressed mice (Fig. 6A–E). Interestingly, there were no significant difference in tau accumulation between

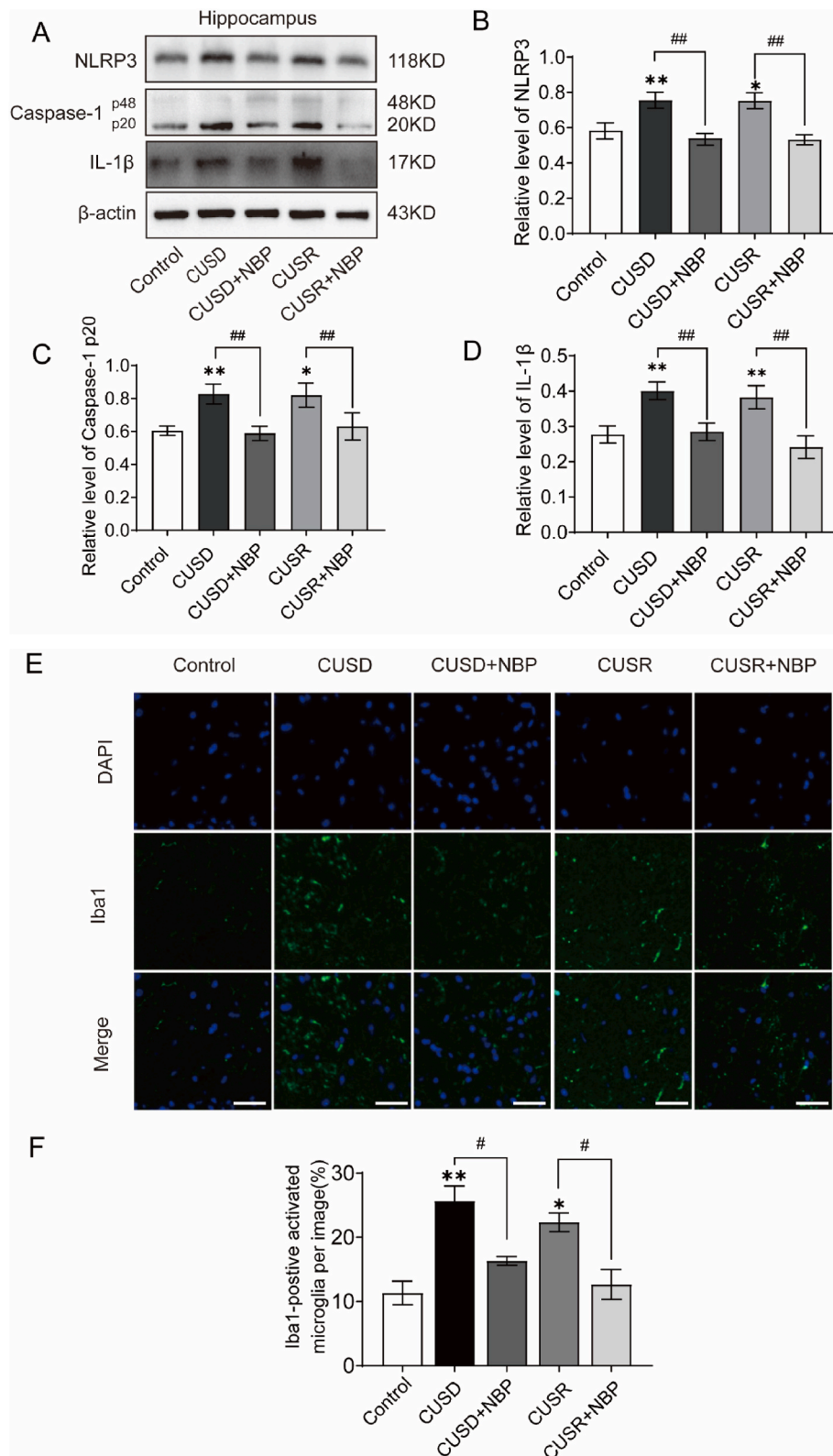


Fig. 3. NBP suppressed NLRP3 inflammasome activation in chronic stress mice
A-D. Western blot and quantification of NLRP3, caspase-1p20, and cleaved IL-1β in the hippocampus lysates. (n = 3, 3, 3, 3, and 3 for group Con, CUSD, CUSD + NBP, CUSR, and CUSR + NBP mice respectively. NLRP3: [Con CUSD] **P = 0.053, [Con CUSR] **P = 0.0057, [CUSD CUSD + NBP] ###P = 0.0041, [CUSR CUSR + NBP] ###P = 0.0054. Caspase-1p20: [Con CUSD] **P = 0.0057, [Con CUSR] *P = 0.0104, [CUSD CUSD + NBP] ###P = 0.0030, [CUSR CUSR + NBP] ###P = 0.0026. IL-1β: [Con CUSD] **P = 0.0012, [Con CUSR] **P = 0.0041, [CUSD CUSD + NBP] ###P = 0.0020, [CUSR CUSR + NBP] ###P = 0.0042.) E. Immunofluorescence of Iba1 (green) in the hippocampus. Scale bar: 100 μm. F. Quantification of E. (n = 3, 3, 3, 3, and 3 for group Con, CUSD, CUSD + NBP, CUSR, CUSR + NBP mice respectively. [Con CUSD] **P = 0.0018, [Con CUSR] *P = 0.0117, [CUSD CUSD + NBP] #P = 0.0314, [CUSR CUSR + NBP] #P = 0.0257. *P < 0.05, **P < 0.01, ##P < 0.05, ###P < 0.01, ####P < 0.001, *P versus Con group, #P versus CUSD or CUSR group. All data are represented by the mean ± SEM. One-way ANOVA with Tukey's multiple comparisons test.).

stressed and non-stressed NLRP3 KO mice (Fig. 6A–E). And compared with the control, the level of p-GSK-3β/GSK-3β was markedly decreased in wild-type mice with CUMS treatment. Similarly, p-GSK-3β/GSK-3β was no significant difference in NLRP3 KO mice (Fig. 6F and G).

We examined synapse-associated proteins (PSD93 and PSD95) in the hippocampus using western-blot. Compared with the control, an

increased level of PSD93 and PSD95 was found in the hippocampus in stressed mice (Fig. 6I–J). In addition, there were no visible bands in either stressed or non-stressed NLRP3 KO mice (Fig. 6I–J).

We also examined the dendritic spine structure in the hippocampus using Golgi staining. We found that the AO and BS spine densities were significantly lower in the CUMS group than those in the wild type group

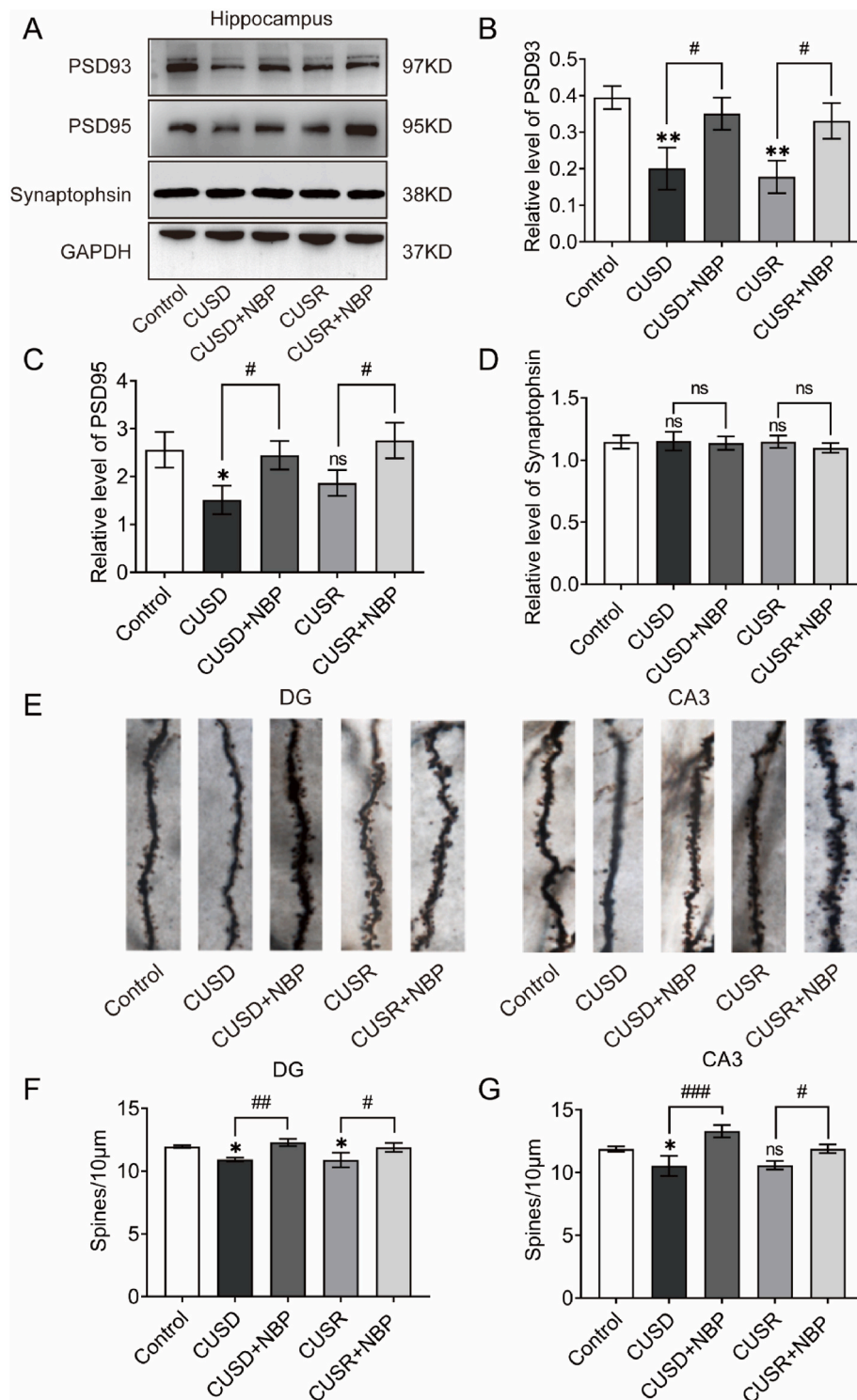


Fig. 4. NBP ameliorates synaptic plasticity impairment caused by chronic stress
A-D. Western blot and quantification of PSD93, PSD95, and Synaptophysin in the hippocampus lysates. (n = 3, 3, 3, and 3 for group Con, CUSD, CUSD + NBP, CUSR, and CUSR + NBP mice respectively. PSD93: [Con CUSD] **P = 0.0029, [Con CUSR] **P = 0.0013, [CUSD CUSD + NBP] #P = 0.0169, [CUSR CUSR + NBP] #P = 0.0148. PSD95: [Con CUSD] *P = 0.0181, [Con CUSR] P = 0.1408, [CUSD CUSD + NBP] #P = 0.0347, [CUSR CUSR + NBP] #P = 0.0459, Synaptophysin: [Con CUSD] P > 0.99, [Con CUSR] P > 0.99, [CUSD CUSD + NBP] P = 0.994, [CUSR CUSR + NBP] P = 0.9649.) E-G. Analysis of dendritic spines (number of spines per unit area) in the hippocampus's DG granule and CA1 pyramidal neurons. (DG: [Con CUSD] *P = 0.0274, [Con CUSR] *P = 0.0219, [CUSD CUSD + NBP] ###P = 0.0444, [CUSR CUSR + NBP] #P = 0.0302. CA3: [Con CUSD] *P = 0.0428, [Con CUSR] P = 0.0513, [CUSD CUSD + NBP] ###P = 0.0003, [CUSR CUSR + NBP] #P = 0.0483. *P < 0.05, **P < 0.01, #P < 0.05, ##P < 0.01, ###P < 0.001, *P versus Con group, #P versus CUSD or CUSR group. All data are represented by the mean ± SEM. One-way ANOVA with Tukey's multiple comparisons test.)

(Fig. 6K and L). No significant difference was found between stressed NLRP3 KO mice and non-stressed NLRP3 KO mice in dendritic spine structure (Fig. 6K and L).

4. Discussion

Hans Selye is the first person to define stress: "Stress is the nonspecific response of the body to any demand" (Fink, 2017). The influence of chronic stress on the development of various mental disorders has been an area of interest along with time. In particular, the strong effect that

chronic stress has on a significantly increased risk for developing depressive and dementia disorders has been the focus of extensive research. However, the mechanism of SICD remain unclear. In this study, we found that both depressive and resilient mice displayed spatial memory deficits and an accumulation of tau in the hippocampus. CUMS could activate NLRP3 inflammasome and destroy synapse structure. Meanwhile, NBP treatment or down-regulation of NLRP3 could significantly inhibit neuroinflammation, ameliorate synaptic dysfunction and cognitive impairment induced by CUMS.

Studies found that the development of anxiety was caused by

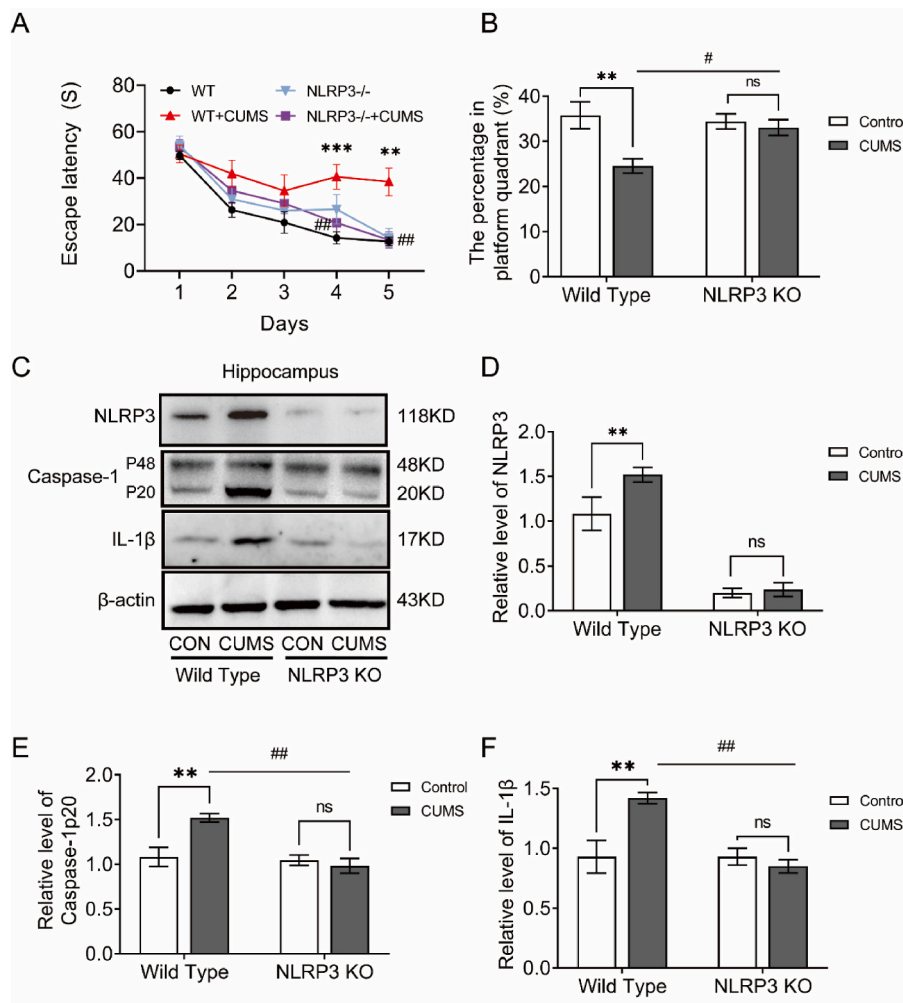


Fig. 5. The behavior alteration in NLRP3 KO mice after CUMS

A-B. Spatial learning and memory test using the acquisition phase. (A) Probe test at consecutive 6 days. (B) MWM test in consecutive 5 days. (n = 7, 8, 8, and 6 for group Con, CUMS, NLRP3^{-/-}, and NLRP3^{-/-} + CUMS, respectively. Escape latency: day4 [Con CUMS] ***P = 0.0008, [CUMS NLRP3^{-/-} + CUMS] ##P = 0.0014, day5: [Con CUMS] **P = 0.0012, [CUMS NLRP3^{-/-} + CUMS] ##P = 0.0027. The percentage in platform quadrant (%): [Con CUMS] **P = 0.0052, [NLRP3^{-/-} NLRP3^{-/-} + CUMS] P > 0.99, [CUMS NLRP3^{-/-} + CUMS] #P = 0.03 stress × genotype interaction F_{1,25} = 4.967, P = 0.0351, two-way ANOVA followed by Bonferroni multiple comparison test.) C-F. Western blot and quantification of NLRP3, caspase-1p20, and cleaved IL-1β in the hippocampus lysates. (n = 3, 3, 3, and 3 for group Con, CUMS, NLRP3^{-/-}, and NLRP3^{-/-} + CUMS, respectively. NLRP3: [Con CUMS] **P = 0.0027, [NLRP3^{-/-} NLRP3^{-/-} + CUMS] P > 0.99, [CUMS NLRP3^{-/-} + CUMS] ##P = 0.0027 stress × genotype interaction F_{1,8} = 10.45, P = 0.012. Caspase-1p20: [Con CUMS] **P = 0.008, [NLRP3^{-/-} NLRP3^{-/-} + CUMS] P = 0.8224, [CUMS NLRP3^{-/-} + CUMS] ##P = 0.0024 stress × genotype interaction F_{1,8} = 10.45, P = 0.012. IL-1β: [Con CUMS] **P = 0.0070, [NLRP3^{-/-} NLRP3^{-/-} + CUMS] P > 0.99, [CUMS NLRP3^{-/-} + CUMS] ##P = 0.0029 stress × genotype interaction F_{1,8} = 11.28, P = 0.01. **P < 0.01, ***P < 0.001, #P < 0.05, ##P < 0.01, *P versus Con group, #P versus CUMS group. All data are represented by the mean ± SEM. Multiple comparisons differences were calculated using two-way ANOVA with Bonferroni's multiple comparisons test.)

increased IL-1β expression and microglia recruitment following the repeated social defeat, and microglial inhibition and depletion significantly alleviated anxiety-like behavior (McKim et al., 2018; Li et al., 2021). Moreover, the maturation and release of IL-1β are mainly regulated by NLRP3. NLRP3 inflammasomes, activated by various types of pathogens or stressors, play a key role in many diseases, including depression (Sharma and Kanneganti, 2021).

However, whether the NLRP3 involve in SICD or not is unclear. Several lines of evidence pointed out the NLRP3 inflammasome activation as a key player in the pathophysiological process of AD. And some researches have shown that inhibiting NLRP3 inflammasome contributed to neuroprotection in AD animal models and patients (Lonnemann et al., 2020; Shippy et al., 2020), implying that NLRP3 inflammasome is vital to cognitive impairment. Our previous study also found that spatial training ameliorates AD-like pathological deficits by reducing NLRP3 inflammasomes in PR5 mice (Ren et al., 2019). Thus, NLRP3 inflammasome has been considered as a therapeutic target for AD. Furthermore, several studies have demonstrated that CUMS can trigger NLRP3 inflammasome activation, which suggested that NLRP3 inflammasome participates in chronic stress-induced depressive-like behaviors. However, these studies in which stressed mice were not subdivided into CUSD and CUSR groups (Yue et al., 2017; Feng et al., 2019). It means that chronic stress can cause the activation of NLRP3 inflammasome in all stressed animals. In the present study, we found that NLRP3 inflammasome is activated in both stress susceptible and resilient mice. Furthermore, both depressive and resilient mice displayed spatial memory deficits and the depressive-like behaviors were observed only in

susceptible group. Altogether, these results suggested that activation of NLRP3 inflammasome mediates the cognitive deficits but not depressive-like behaviors in CUMS mice. NBP could alleviate the activation of NLRP3 inflammasome in accompany with improvement of cognitive function. Meanwhile, deletion of NLRP3 could significantly inhibit neuroinflammation, ameliorate cognitive impairment induced by CUMS, suggesting that NLRP3 inflammasome play an important role in SICD.

In accordance with our previous results in CUMS rats (Wu et al., 2018b), in the present study, we also found that both stress susceptible and resilient mice showed impaired cognitive function, which suggest that chronic stress-induced cognitive impairment is not caused by chronic stress-induced emotional impairment. Interestingly, we found that tau accumulation was found in both CUSD and CUSR mice. Numerous studies have demonstrated that NLRP3 inflammasome activation drives tau pathology (Ising et al., 2019; Stancu et al., 2019). In our study, we also found that NLRP3 inflammasome activation was found in CUSD and CUSR mice, NBP could alleviate the activation of NLRP3 inflammasome and decreased tau accumulation in CUMS mice. And abnormal tau accumulation was not found in NLRP3 knock out mice. Altogether, our results suggested that the tau pathology induced by CUMS was caused by NLRP3 inflammasome activation. Furthermore, recent studies have also shown that tau knockout mice do not exhibit stress-induced pathological behaviors and atrophy of hippocampal dendrites or deficits of hippocampal connectivity, implicated that tau was an essential mediator of the adverse effects of stress on brain structure and function (Lopes et al., 2016). In accordance with our

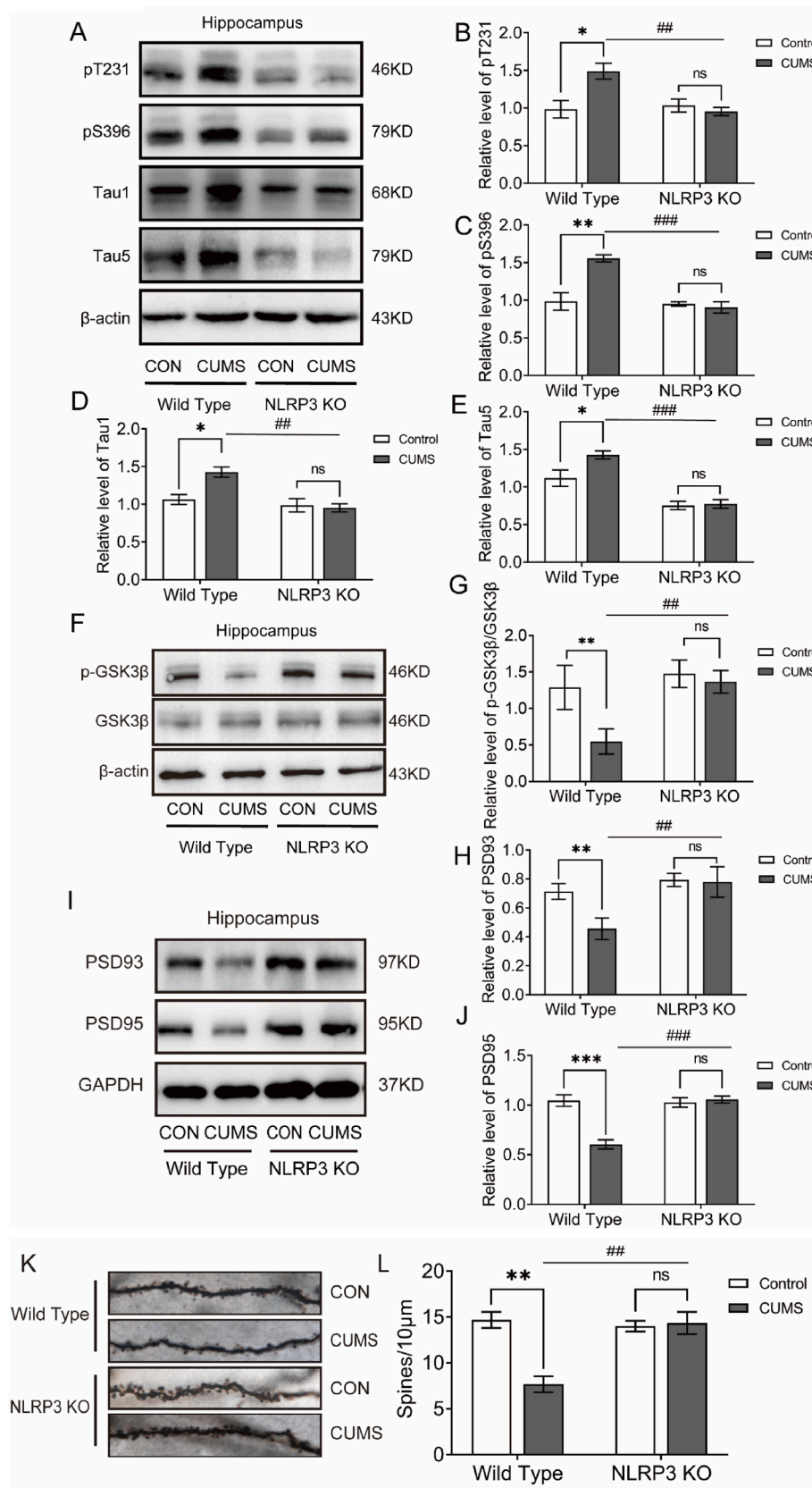


Fig. 6. The pathological alteration in NLRP3 KO mice after CUMS

A-J. Western blot and quantification of pT231, pS396, Tau1, Tau5, p-GSK3β, GSK3β, PSD93, and PSD95 in the hippocampus lysates. (n = 3, 3, 3 and 3 for group Con, CUMS, NLRP3^{-/-}, and NLRP3^{-/-} + CUMS, respectively. pT231: [Con CUMS] *P = 0.0105, [NLRP3^{-/-} NLRP3^{-/-} + CUMS] P > 0.99, [CUMS NLRP3^{-/-} + CUMS] ###P = 0.0077 stress × genotype interaction F_{1,8} = 9.668, P = 0.0145. pS396: [Con CUMS] **P = 0.0013, [NLRP3^{-/-} NLRP3^{-/-} + CUMS] P > 0.99, [CUMS NLRP3^{-/-} + CUMS] ###P = 0.0005 stress × genotype interaction F_{1,8} = 17.14, P = 0.0033. Tau1: [Con CUMS] *P = 0.0133, [NLRP3^{-/-} NLRP3^{-/-} + CUMS] P = 0.9364, [CUMS NLRP3^{-/-} + CUMS] ##P = 0.0030 stress × genotype interaction F_{1,8} = 7.850, P = 0.0231. Tau5: [Con CUMS] *P = 0.0236, [NLRP3^{-/-} NLRP3^{-/-} + CUMS] P = 0.9214, [CUMS NLRP3^{-/-} + CUMS] ###P = 0.0007 stress × genotype interaction F_{1,8} = 6.524, P = 0.0339. p-GSK3β/GSK3β: [Con CUMS] **P = 0.0053, [NLRP3^{-/-} NLRP3^{-/-} + CUMS] P > 0.99, [CUMS NLRP3^{-/-} + CUMS] ##P = 0.0030 stress × genotype interaction F_{1,8} = 6.660, P = 0.0326. PSD93: [Con CUMS] **P = 0.0051, [NLRP3^{-/-} NLRP3^{-/-} + CUMS] P = 0.9698, [CUMS NLRP3^{-/-} + CUMS] ##P = 0.0013 stress × genotype interaction F_{1,8} = 8.354, P = 0.0202. PSD95: [Con CUMS] ***P = 0.0004, [NLRP3^{-/-} NLRP3^{-/-} + CUMS] P > 0.99, [CUMS NLRP3^{-/-} + CUMS] ###P = 0.0003 stress × genotype interaction F_{1,8} = 24.49, P = 0.0011. Two-way ANOVA followed by Bonferroni multiple comparison test) K-L. Analysis of dendritic spines (number of spines per unit area) in neurons of the hippocampus. (n = 3, 3, 3, and 3 for group Con, CUMS, NLRP3^{-/-}, and NLRP3^{-/-} + CUMS, respectively. [Con CUMS] **P = 0.0013, [NLRP3^{-/-} NLRP3^{-/-} + CUMS] P > 0.99, [CUMS NLRP3^{-/-} + CUMS] ##P = 0.0017 stress × genotype interaction F_{1,8} = 16.13, P = 0.0039. *P < 0.05, **P < 0.01, ***P < 0.001, ##P < 0.01, ###P < 0.001, *P versus Con group, #P versus CUMS group. All data are represented by the mean ± SEM. Multiple comparisons differences were calculated using two-way ANOVA with Bonferroni's multiple comparisons test.).

previous studies, our results implied that stress-induced tau accumulation could be a potential mechanism for the observed cognitive deficits in both susceptible and resilient groups.

Previous research has indicated that abnormal accumulation of tau protein contributes to disturbance of neural plasticity in AD (Shao et al., 2011). Synapses are the functional units of neuronal communication, and synaptic dysfunction is directly linked to cognitive disturbances (Singh et al., 2019; Peng et al., 2022). Synaptic impairment is likely to be the major contributor to memory loss in AD (Arendt, 2009; Barthelet and Mülle, 2020). In our study, we found that compared with the control group, the expression of synaptic markers (PSD95, PSD93) and the number of dendritic spines were decreased both in CUSR and CUSD group. Dendritic spines are tiny protrusions of dendrites that are essential for excitatory synaptic transmission (Spruston, 2008). Thus, these structural changes will lead to cognitive dysfunction. Numerous studies have provided evidence that decreased levels of IL-1 β could improve synaptic structure and function in AD mice (Zhang et al., 2021; Patterson, 2015). Our previous study also found that the NLRP3/caspase-1/IL-1 β axis plays an important role in regulating synaptic plasticity (Ren et al., 2019). In the present study, we found that CUMS could activate NLRP3 inflammasome, in accordance with synaptic impairment and memory deficits, furthermore, deletion of NLRP3 could significantly alleviate synaptic impairment and memory deficits, suggesting that synaptic function regulated by NLRP3 inflammasome play an important role in SICD.

NBP, which has been widely used to treat ischemic patients in clinical practice, have been also found to provide a neuroprotection effect on patients with radiation-induced brain injury (Zhang et al., 2017). Many preclinical studies found that NBP rescues hippocampal synaptic failure and attenuates neuropathology in AD (Huang et al., 2021). In addition to antioxidant property and autophagic mechanism, recent researches have suggested a neuroprotection role of NBP via inhibiting microglial activation in rats following traumatic spinal cord injury (He et al., 2017) and in mouse injected with LPS (Chen et al., 2018). Wang and colleagues identified that NBP treatment suppressed the activation of NLRP3 inflammasomes to alleviate neuroinflammation in the APP/PS1 mouse brain (Wang et al., 2019). In the present study, we found that CUMS could activate NLRP3 inflammasome, destruct synaptic structure, induce tau accumulation in the brain and decrease cognitive function in mice. NBP could significantly inhibit the activation of NLRP3 inflammasome, ameliorate synaptic dysfunction, tau accumulation and cognitive impairment induced by CUMS. Furthermore, we also found that deletion of NLRP3 could both significantly inhibit neuroinflammation, ameliorate synaptic dysfunction and cognitive impairment induced by CUMS. Taken together, our results suggest that NBP ameliorates cognitive impairments and selectively attenuates phosphorylated tau accumulation in stressed mice through the regulation of NLRP3 inflammatory signaling pathway.

In summary, our results demonstrated that NLRP3/caspase-1/IL-1 β axis play a pivotal role in SICD and NBP ameliorates cognitive impairments and selectively attenuates phosphorylated tau accumulation through the regulation of NLRP3 inflammatory signaling pathway.

Competing interests

The authors declare that they have no competing interests associated with the manuscript.

CRedit authorship contribution statement

Xiu Chen: carried out the experiments, Formal analysis, performed statistical analyses, Data curation, Writing – original draft, analyzed the data and wrote the manuscript. All authors edited and approved the final version of the manuscript. **Juan-Ling He:** carried out the experiments, Formal analysis, performed statistical analyses, Data curation, Writing – original draft, analyzed the data and wrote the manuscript. All authors

edited and approved the final version of the manuscript. **Xue-Ting Liu:** carried out the experiments, Formal analysis, performed statistical analyses, Data curation, Writing – original draft, analyzed the data and wrote the manuscript. All authors edited and approved the final version of the manuscript. **Na Zhao:** carried out the experiments. All authors edited and approved the final version of the manuscript. **Fan Geng:** carried out the experiments. All authors edited and approved the final version of the manuscript. **Meng-Meng Zhu:** carried out the experiments. All authors edited and approved the final version of the manuscript. **Gong-Ping Liu:** Conceptualization, Project administration, contributed to the research concept, research administration and support. All authors edited and approved the final version of the manuscript. **Qing-Guo Ren:** Conceptualization, Project administration, contributed to the research concept, research administration and support. All authors edited and approved the final version of the manuscript.

Acknowledgments

This research was supported by the National Natural Science Foundation of China (81870850).

References

- Arendt, T., 2009. Synaptic degeneration in Alzheimer's disease. *Acta Neuropathol.* 118, 167–179. <https://doi.org/10.1007/s00401-009-0536-x>.
- Barrett, T.J., Corr, E.M., van Solingen, C., et al., 2021. Chronic stress primes innate immune responses in mice and humans. *Cell Rep.* 36, 109595 <https://doi.org/10.1016/j.celrep.2021.109595>.
- Barthelet, G., Mülle, C., 2020. Presynaptic failure in Alzheimer's disease. *Prog. Neurobiol.* 194, 101801 <https://doi.org/10.1016/j.pneurobio.2020.101801>.
- Bhattacharya, A., Derecki, N.C., Lovenberg, T.W., Drevets, W.C., 2016. Role of neuro-immunological factors in the pathophysiology of mood disorders. *Psychopharmacology* 233, 1623–1636. <https://doi.org/10.1007/s00213-016-4214-0>.
- Chen, Y., Jiang, M., Li, L., et al., 2018. DL-3-n-butylphthalide reduces microglial activation in lipopolysaccharide-induced Parkinson's disease model mice. *Mol. Med. Rep.* 17, 3884–3890. <https://doi.org/10.3892/mmr.2017.8332>.
- Crump, C., Sundquist, K., Winkleby, M.A., Sundquist, J., 2013. Mental disorders and risk of accidental death. *Br. J. Psychiatry* 203, 297–302. <https://doi.org/10.1192/bjp.bp.112.123992>.
- DiSabato, D.J., Nemeth, D.P., Liu, X., et al., 2021. Interleukin-1 receptor on hippocampal neurons drives social withdrawal and cognitive deficits after chronic social stress. *Mol. Psychiatr.* 26, 4770–4782. <https://doi.org/10.1038/s41380-020-0788-3>.
- Fan, X., Shen, W., Wang, L., Zhang, Y., 2021. Efficacy and safety of DL-3-n-butylphthalide in the treatment of poststroke cognitive impairment: a systematic review and meta-analysis. *Front. Pharmacol.* 12, 810297 <https://doi.org/10.3389/fphar.2021.810297>.
- Feng, X., Zhao, Y., Yang, T., et al., 2019. Glucocorticoid-driven NLRP3 inflammasome activation in hippocampal microglia mediates chronic stress-induced depressive-like behaviors. *Front. Mol. Neurosci.* 12, 210. <https://doi.org/10.3389/fnmol.2019.00210>.
- Fink, G., 2017. Stress: concepts, definition and history. In *Reference Module Neuroscience and Biobehavioral Psychology*, Elsevier Inc., Amsterdam, 1–9.
- Gao, S., Wang, X., Meng, L.B., et al., 2022. Recent progress of chronic stress in the development of atherosclerosis. *Oxid. Med. Cell. Longev.* 2022, 4121173 <https://doi.org/10.1155/2022/4121173>.
- Greenberg, M.S., Tanev, K., Marin, M.F., Pitman, R.K., 2014. Stress, PTSD, and dementia. *Alzheimers Dement* 10, S155–S165. <https://doi.org/10.1016/j.jalz.2014.04.008>.
- He, Z., Zhou, Y., Lin, L., et al., 2017. DL-3-n-butylphthalide attenuates acute inflammatory activation in rats with spinal cord injury by inhibiting microglial TLR4/NF- κ B signalling. *J. Cell Mol. Med.* 21, 3010–3022. <https://doi.org/10.1111/jcmm.13212>.
- Heneka, M.T., McManus, R.M., Latz, E., 2018. Inflammasome signalling in brain function and neurodegenerative disease. *Nat. Rev. Neurosci.* 19, 610–621. <https://doi.org/10.1038/s41583-018-0055-7>.
- Huang, L., Lan, J., Tang, J., et al., 2021. L-3-n-Butylphthalide improves synaptic and dendritic spine plasticity and ameliorates neurite pathology in Alzheimer's disease mouse model and cultured hippocampal neurons. *Mol. Neurobiol.* 58, 1260–1274. <https://doi.org/10.1007/s12035-020-02183-y>.
- Ising, C., Venegas, C., Zhang, S., et al., 2019. NLRP3 inflammasome activation drives tau pathology. *Nature* 575, 669–673. <https://doi.org/10.1038/s41586-019-1769-z>.
- Karp, N.A., Meehan, T.F., Morgan, H., et al., 2015. Applying the ARRIVE guidelines to an in vivo database. *PLoS Biol.* 13, e1002151 <https://doi.org/10.1371/journal.pbio.1002151>.
- Kim, J.J., Diamond, D.M., 2002. The stressed hippocampus, synaptic plasticity and lost memories. *Nat. Rev. Neurosci.* 3, 453–462. <https://doi.org/10.1038/nrn849>.

- Knezevic, D., Mizrahi, R., 2018. Molecular imaging of neuroinflammation in Alzheimer's disease and mild cognitive impairment. *Prog. Neuro-Psychopharmacol. Biol. Psychiatry* 80, 123–131. <https://doi.org/10.1016/j.pnpbp.2017.05.007>.
- Li, S., Liao, Y., Dong, Y., et al., 2021. Microglial deletion and inhibition alleviate behavior of post-traumatic stress disorder in mice. *J. Neuroinflammation* 18, 7. <https://doi.org/10.1186/s12974-020-02069-9>.
- Liu, M.Y., Yin, C.Y., Zhu, L.J., et al., 2018. Sucrose preference test for measurement of stress-induced anhedonia in mice. *Nat. Protoc.* 13, 1686–1698. <https://doi.org/10.1038/s41596-018-0011-z>.
- Liu, X., Liu, R., Fu, D., et al., 2021 Jan 10. DL-3-n-butylphthalide inhibits neuroinflammation by stimulating foxp3 and Ki-67 in an ischemic stroke model. *Aging (Albany NY)* 13 (3), 3763–3778. <https://doi.org/10.18632/aging.202338>.
- Lonnemann, N., Hosseini, S., Marchetti, C., et al., 2020. The NLRP3 inflammasome inhibitor OLT1177 rescues cognitive impairment in a mouse model of Alzheimer's disease. *Proc. Natl. Acad. Sci. U. S. A.* 117, 32145–32154. <https://doi.org/10.1073/pnas.2009680117>.
- Lopes, S., Vaz-Silva, J., Pinto, V., et al., 2016. Tau protein is essential for stress-induced brain pathology. *Proc. Natl. Acad. Sci. U. S. A.* 113, E3755–E3763. <https://doi.org/10.1073/pnas.1600953113>.
- Lotan, A., Lifschytz, T., Wolf, G., et al., 2018. Differential effects of chronic stress in young-adult and old female mice: cognitive-behavioral manifestations and neurobiological correlates. *Mol. Psychiatr.* 23, 1432–1445. <https://doi.org/10.1038/mp.2017.237>.
- Lu, M., Yang, J.Z., Geng, F., Ding, J.H., Hu, G., 2014. Iptakalim confers an antidepressant effect in a chronic mild stress model of depression through regulating neuroinflammation and neurogenesis. *Int. J. Neuropsychopharmacol.* 17, 1501–1510. <https://doi.org/10.1017/s1461145714000285>.
- Marco-Contelles, J., Zhang, Y., 2020. From seeds of Apium graveolens linn. To a cerebral ischemia medicine: the long journey of 3-n-Butylphthalide. *J. Med. Chem.* 63, 12485–12510. <https://doi.org/10.1021/acs.jmedchem.0c00887>.
- McKim, D.B., Niraula, A., Tarr, A.J., Wohleb, E.S., Sheridan, J.F., Godbout, J.P., 2016. Neuroinflammatory dynamics underlie memory impairments after repeated social defeat. *J. Neurosci. : Off. J. Soc. Neurosci.* 36, 2590–2604. <https://doi.org/10.1523/jneurosci.2394-15.2016>.
- McKim, D.B., Weber, M.D., Niraula, A., et al., 2018. Microglial recruitment of IL-1 β -producing monocytes to brain endothelium causes stress-induced anxiety. *Mol. Psychiatr.* 23, 1421–1431. <https://doi.org/10.1038/mp.2017.64>.
- Ning, L.N., Zhang, T., Chu, J., et al., 2018. Gender-related hippocampal proteomics study from young rats after chronic unpredictable mild stress exposure. *Mol. Neurobiol.* 55, 835–850. <https://doi.org/10.1007/s12035-016-0352-y>.
- Patterson, S.L., 2015. Immune dysregulation and cognitive vulnerability in the aging brain: interactions of microglia, IL-1 β , BDNF and synaptic plasticity. *Neuropharmacology* 96, 11–18. <https://doi.org/10.1016/j.neuropharm.2014.12.020>.
- Peng, Y., Sun, J., Hon, S., et al., 2010. L-3-n-butylphthalide improves cognitive impairment and reduces amyloid-beta in a transgenic model of Alzheimer's disease. *J. Neurosci. : Off. J. Soc. Neurosci.* 30, 8180–8189. <https://doi.org/10.1523/JNEUROSCI.0340-10.2010>.
- Peng, L., Bestard-Lorigados, L., Song, W., 2022. The synapse as a treatment avenue for Alzheimer's Disease. *Mol. Psychiatr.* <https://doi.org/10.1038/s41380-022-01565-z>.
- Percie du Sert, N., Ahluwalia, A., Alam, S., et al., 2020. Reporting animal research: explanation and elaboration for the ARRIVE guidelines 2.0. *PLoS Biol.* 18, e3000411. <https://doi.org/10.1371/journal.pbio.3000411>.
- Porsolt, R.D., Le Pichon, M., Jalfre, M., 1977. Depression: a new animal model sensitive to antidepressant treatments. *Nature* 266, 730–732. <https://doi.org/10.1038/266730a0>.
- Que, R., Zheng, J., Chang, Z., et al., 2021. DL-3-n-Butylphthalide rescues dopaminergic neurons in Parkinson's disease models by inhibiting the NLRP3 inflammasome and ameliorating mitochondrial impairment. *Front. Immunol.* 12, 794770. <https://doi.org/10.3389/fimmu.2021.794770>.
- Ren, Q.G., Gong, W.G., Zhou, H., Shu, H., Wang, Y.J., Zhang, Z.J., 2019. Spatial training ameliorates long-term Alzheimer's disease-like pathological deficits by reducing NLRP3 inflammasomes in PR5 mice. *Neurotherapeutics* 16, 450–464. <https://doi.org/10.1007/s13311-018-00698-w>.
- Russell, G., Lightman, S., 2019. The human stress response. *Nat. Rev. Endocrinol.* 15, 525–534. <https://doi.org/10.1038/s41574-019-0228-0>.
- Sanacora, G., Yan, Z., Popoli, M., 2022 Feb. The stressed synapse 2.0: pathophysiological mechanisms in stress-related neuropsychiatric disorders. *Nat. Rev. Neurosci.* 23 (2), 86–103. <https://doi.org/10.1038/s41583-021-00540-x>.
- Setiawan, E., Wilson, A.A., Mizrahi, R., et al., 2015. Role of translocator protein density, a marker of neuroinflammation, in the brain during major depressive episodes. *JAMA Psychiatr.* 72, 268–275. <https://doi.org/10.1001/jamapsychiatry.2014.2427>.
- Shao, C.Y., Mirra, S.S., Sait, H.B., Sacktor, T.C., Sigurdsson, E.M., 2011. Postsynaptic degeneration as revealed by PSD-95 reduction occurs after advanced A β and tau pathology in transgenic mouse models of Alzheimer's disease. *Acta Neuropathol.* 122, 285–292. <https://doi.org/10.1007/s00401-011-0843-x>.
- Sharma, B.R., Kanneganti, T.D., 2021. NLRP3 inflammasome in cancer and metabolic diseases. *Nat. Immunol.* 22, 550–559. <https://doi.org/10.1038/s41590-021-00886-5>.
- Shippy, D.C., Wilhelm, C., Viharkumar, P.A., Raife, T.J., Ulland, T.K., 2020. β -Hydroxybutyrate inhibits inflammasome activation to attenuate Alzheimer's disease pathology. *J. Neuroinflammation* 17, 280. <https://doi.org/10.1186/s12974-020-01948-5>.
- Singh, B., Covelo, A., Martell-Martínez, H., et al., 2019. Tau is required for progressive synaptic and memory deficits in a transgenic mouse model of α -synucleinopathy. *Acta Neuropathol.* 138, 551–574. <https://doi.org/10.1007/s00401-019-02032-w>.
- Spruston, N., 2008. Pyramidal neurons: dendritic structure and synaptic integration. *Nat. Rev. Neurosci.* 9, 206–221. <https://doi.org/10.1038/nrn2286>.
- Stancu, I.C., Cremers, N., Vanrusselt, H., et al., 2019. Aggregated Tau activates NLRP3-ASC inflammasome exacerbating exogenously seeded and non-exogenously seeded Tau pathology in vivo. *Acta Neuropathol.* 137, 599–617. <https://doi.org/10.1007/s00401-018-01957-y>.
- Vorhees, C.V., Williams, M.T., 2006. Morris water maze: procedures for assessing spatial and related forms of learning and memory. *Nat. Protoc.* 1, 848–858. <https://doi.org/10.1038/nprot.2006.116>.
- Wang, C.Y., Xu, Y., Wang, X., Guo, C., Wang, T., Wang, Z.Y., 2019. DL-3-n-Butylphthalide inhibits NLRP3 inflammasome and mitigates Alzheimer's-like pathology via Nrf2-TXNIP-Trx Axis. *Antioxidants Redox Signal.* 30, 1411–1431. <https://doi.org/10.1089/ars.2017.7440>.
- Wang, B.N., Wu, C.B., Chen, Z.M., et al., 2021. DL-3-n-butylphthalide ameliorates diabetes-associated cognitive decline by enhancing PI3K/Akt signaling and suppressing oxidative stress. *Acta Pharmacol. Sin.* 42, 347–360. <https://doi.org/10.1038/s41401-020-00583-3>.
- Wilson, R.S., Evans, D.A., Bienias, J.L., Mendes de Leon, C.F., Schneider, J.A., 2003 Dec 9. Bennett. DA. Proneness to psychological distress is associated with risk of Alzheimer's disease. *Neurology* 61 (11), 1479–1485. <https://doi.org/10.1212/01.WNL.0000096167.56734.59>.
- Wu, C., Gong, W.G., Wang, Y.J., et al., 2018a. Escitalopram alleviates stress-induced Alzheimer's disease-like tau pathologies and cognitive deficits by reducing hypothalamic-pituitary-adrenal axis reactivity and insulin/GSK-3 β signal pathway activity. *Neurobiol. Aging* 67, 137–147. <https://doi.org/10.1016/j.neurobiolaging.2018.03.011>.
- Wu, C., Gong, W.G., Wang, Y.J., et al., 2018b. Escitalopram alleviates stress-induced Alzheimer's disease-like tau pathologies and cognitive deficits by reducing hypothalamic-pituitary-adrenal axis reactivity and insulin/GSK-3 β signal pathway activity. *Neurobiol. Aging* 67, 137–147. <https://doi.org/10.1016/j.neurobiolaging.2018.03.011>.
- Wu, F., Xu, K., Xu, K., et al., 2020. DL-3n-butylphthalide improves traumatic brain injury recovery via inhibiting autophagy-induced blood-brain barrier disruption and cell apoptosis. *J. Cell Mol. Med.* 24, 1220–1232. <https://doi.org/10.1111/jcmm.14691>.
- Wu, A.G., Zhou, X.G., Qiao, G., et al., 2021. Targeting microglial autophagic degradation in NLRP3 inflammasome-mediated neurodegenerative diseases. *Ageing Res. Rev.* 65, 101202. <https://doi.org/10.1016/j.arr.2020.101202>.
- Xiang, H., Zhang, Q., Han, Y., et al., 2021. Novel brain-targeting 3-n-butylphthalide prodrugs for ischemic stroke treatment. *J. Contr. Release* 335, 498–514. <https://doi.org/10.1016/j.jconrel.2021.05.045>.
- Yue, N., Huang, H., Zhu, X., et al., 2017. Activation of P2X7 receptor and NLRP3 inflammasome assembly in hippocampal glial cells mediates chronic stress-induced depressive-like behaviors. *J. Neuroinflammation* 14, 102. <https://doi.org/10.1186/s12974-017-0865-y>.
- Zhang, X., Li, Y., Li, X., Rong, X., Tang, Y., Peng, Y., 2017. Neuroprotective effect of DL-3-n-butylphthalide on patients with radiation-induced brain injury: a clinical retrospective cohort study. *Int. J. Neurosci.* 127, 1059–1064. <https://doi.org/10.1080/00207454.2017.1310727>.
- Zhang, B., Lian, W., Zhao, J., Wang, Z., Liu, A., Du, G., 2021. DL0410 alleviates memory impairment in D-galactose-induced aging rats by suppressing neuroinflammation via the TLR4/MyD88/NF- κ B pathway. *Oxid. Med. Cell. Longev.* 2021, 6521146. <https://doi.org/10.1155/2021/6521146>.